

# Optimisation of Drilling Parameters of SiC<sub>p</sub> Reinforced Al-2024 Composite used in Aircraft Industry

Ferit Ficici

Department of Development and Research, Global Arge, Kocaeli 41400, Turkey

Received 04 February 2024; revised 23 September 2024; accepted 10 March 2025

In this research, the machinability characteristics of Al-2024 + SiC composite materials produced via the stir casting method were experimentally analyzed. The test samples included unreinforced composites and those with 5%, 10%, and 15% SiC particle reinforcement. Microstructural examinations were conducted using optical and Scanning Electron Microscopes (SEM). Hardness measurements were taken using the Brinell scale. Machinability tests involved drilling on a 3-axis CNC machine with both HSS and HSS + TiN drill bits, using three different feed rates and cutting speeds. The unreinforced sample exhibited the lowest hardness, while the sample with 15% SiC reinforcement showed the highest hardness. The HSS + TiN drill bit outperformed the HSS drill bit. Thrust force and torque values increased with higher feed rates and cutting speeds. ANOVA statistical analysis indicated that the drill type (variable A) influenced thrust force by 58.36%, the composite type (variable D) by 31.25%, and cutting speed (variable C) by 7.64%. For torque, the composite type (variable D) had a 55.94% influence, the drill type (variable A) 24.96%, and cutting speed (variable C) 13.26%. It was also found that the interaction between variables A and B did not affect cutting forces.

**Keywords:** Al-2024 alloy, Drilling, SiC<sub>p</sub>, Thrust force, Torque

## Introduction

Aluminum Matrix Composite (AMC) with SiC particle reinforcement phase is formed by combining the beneficial properties of both materials. The load on the composite material formed is shared by the aluminum matrix and the SiC particle reinforcement phase. The interface bond strength formed between these two components plays an important role in load transmission. This interface bond strength determines the mechanical properties of the composite material. The interface bond strength depends on factors such as the manufacturing method, reinforcement phase-type, shape, size, ratio and distribution, and physical and chemical compatibility between the matrix and the reinforcement phase.<sup>1</sup>

Many methods are used in the production of AMC. These are stirred casting, powder metallurgy, squeeze casting, deposition technique, and electroplating. One of the most widely used of these techniques is stir casting. The particle reinforcement phase is added to the molten metal and the production is made. In this process, a melt is produced from the matrix material. The reinforcement phase is then added. The composite material is produced by mixing this

mixture with the help of a stirrer and pouring it into pre-prepared molds.<sup>2</sup>

Composite materials are used in aircraft construction over the years. Composite materials have become more attractive in the manufacture of structures where high performance is required, such as aircraft. Its use has gradually increased, especially in Boeing aircraft types. Composite materials have superior mechanical properties, such as higher hardness, fatigue, and corrosion resistance compared to metals.<sup>3,4</sup>

Aluminum 2000 series alloys are the most important alloys used in structural applications such as airframes. These magnesium-containing alloys provide many advantages in their mechanical properties as a result of the precipitation of Al<sub>2</sub>Cu and Al<sub>2</sub>CuMg phases. Compared with other alloy series, they have higher strength, superior damage tolerance, and fatigue cracking resistance. In this series, 2024 alloy is one of the most well-known examples. 2024 aluminum alloy has been one of the alloys used in aircraft and automobile fuselage construction. Al-2024 alloy has mechanical properties such as moderate yield strength, very good resistance to fatigue crack growth, and fracture toughness.<sup>4</sup>

Silicon carbide (SiC) is a compound containing silica and carbon particles. It has many properties,

especially high hardness, strength, low density, and good thermal conductivity. SiC particle reinforcement phases are widely used in the production of aluminum matrix composite materials.<sup>5,6</sup>

The aviation and automotive industries require millions of holes, especially for the riveted and bolted assembly. Therefore, the traditional drilling process is the most important machining process in these sectors. Especially these fasteners are exposed to constant load and vibration during the flight period. In addition, assembly holes are created manually.<sup>7,8</sup> In the drilling process, the drill bit is subjected to high thrust force and temperature. Due to the presence of hard and abrasive reinforcement phases in composite materials, more cutting forces and temperature occurs on the drill during drilling compared to unreinforced aluminum.<sup>9,10</sup>

Drilling factors such as feed rate and cutting speed, material factors such as reinforcement phase ratio, and external factors such as cutting tool type affect cutting forces. Therefore, drilling parameters and cutting tool types should be selected appropriately.

Many studies have been carried out to investigate the effect of input parameters such as drilling feed rate, cutting speed and different drill bits on MMC components. Liu *et al.* proposed an energy-based mechanistic model to predict the cutting force in drilling of SiCp/Al composites, accurately considering the effect of abrasive particles and energy consumption with a margin of error of 6.55%.<sup>11</sup> Zhu *et al.* utilized an improved BP neural network algorithm to accurately predict the drilling force of high-volume SiCp/Al composites, with experimental results confirming the model's consistency across various cutting speeds and feed rates.<sup>12</sup> Abbas *et al.* found that cryogenic treatment of drills significantly enhances the machinability of aluminum-silicon carbide (Al/SiC) composites by increasing drill hardness, reducing thrust force and vibration, and improving surface roughness.<sup>13</sup> Ghalme and Karolczak aimed to optimize drilling parameters for Saffil fiber-reinforced Al MMC under MQL conditions, finding that a drill speed of 11 m/min and a feed rate of 0.05 mm/rev minimize surface roughness, roundness error, and feed force.<sup>14</sup> Sharath *et al.* found that the Al7029/10% B4C-5% Gr hybrid composite, due to graphite's lubricating properties, exhibited reduced thrust force, torque, and burr height compared to the Al7029/10% B4C composite, with carbide tools proving more effective than TiN-coated HSS drill bits for machining these composites.<sup>15</sup> Umer

*et al.* investigated the effects of reinforcement particle size and cutting parameters on machining performance of aluminum-based MMCs, finding that optimal conditions for minimizing surface roughness and tool-chip interface temperature involve moderate cutting speeds, low feed rates, and shallow cuts.<sup>16</sup> The study by Yıldız and Sur optimized drilling parameters for aluminum-oxide-reinforced functionally graded aluminum composites, finding that feed rate significantly impacts thrust force and surface roughness, with the optimal conditions being a 140° point angle, 15° helix angle, and 0.075 mm/rev feed rate.<sup>17</sup> Selvamani *et al.* studied the drilling of aluminum-based hybrid-reinforced metal matrix composites (HMMC) and found that feed rate significantly impacts thrust force and torque, with the performance evaluated based on tool abrasion and machining quantity.<sup>18</sup> Xiang *et al.* developed and validated a mechanism-based diamond wear model for drilling high-volume fraction SiCp/Al6063 composites, identifying dominant wear mechanisms and achieving accurate tool wear estimates through a combined abrasive-chemical subroutine in a 3D drilling FE model.<sup>19</sup> Liu and colleagues examined the impact of particle properties on the mechanical properties of SiCp/Al composites and analyzed both conventional and advanced machining mechanisms, revealing that advanced machining techniques significantly improve processability and identifying future research areas.<sup>20</sup>

As a result of the literature review, it was determined that the researches on the processability of SiC-reinforced Al2024 composite materials are few, and the processing methods observed in the literature require expertise as well as high installation costs. In this study, the process of machinability by drilling was preferred due to the most widely used perforated assembly process in the automotive and aerospace industry. Composite materials were produced using stir casting method. In addition, as another feature of this study, Taguchi and ANOVA statistical methods, which are simple, efficient and systematically powerful in terms of both quality and cost, were used to contribute to the industry and academia. Therefore, the aim of this study is to experimentally and statistically investigate the effect of internal parameters such as cutting speed and feed rate and external parameters such as cutting tool materials and weight ratio of reinforcement phase on cutting forces in the drilling process of pure Al 2024 and SiCp reinforced Al 2024 composite materials.

## Experimental Details

### Materials

In this study, Al-2024 alloy was preferred as a matrix for composite material production. Al-2024 alloy series used in the automobile and aviation industry has many features e.g. lightness, high strength, high strength/weight ratio, good damage resistance, and fatigue strength. The chemical components and mechanical properties of Al-2024 alloy used in this study are given in Table 1.

### Reinforcement Phase

In this study, particle-shaped silicon carbide (SiC) is used as a reinforcement phase in composite material production. The particle sizes of these particles were measured with Microtrac S3500 brand device. The grain size analysis result indicates that the grain size varied between 1  $\mu\text{m}$  and 100  $\mu\text{m}$ , and the average grain size was determined as 20  $\mu\text{m}$ .<sup>21</sup> To have a stronger interface bond between the matrix material and the reinforcement phase in composite materials, the wetting property must be improved. Therefore, the oxidation process has been carried out on the surfaces of SiC particles.

### Composite Production Method

In this study, the stir casting production method was used to produce SiC reinforced Al-2024 composite materials. In this study, aluminum alloy melting was carried out in an induction furnace. This furnace has an aluminum alloy melting capacity of 8 kg. A sufficient amount of Al-2024 alloy is placed in the furnace and the melting process is carried out

by increasing it to 700°C. After melting, the liquid metal is degassed. When the temperature of the alloy is in the range of 630-640°C, 5%, 10%, and 15% by volume of SiC particles are added to the alloy under argon atmosphere. While adding SiC particles, mixing is carried out with the help of a mechanical stirrer. Mixing was done at 900 rpm for 5 minutes. The schematic of the stir casting production method applied in this study is shown in Fig. 1.

### Drilling Test

In this study, the drilling process was used to examine the machinability behavior of SiC reinforced Al-2024 composite materials. For this purpose, experiments were carried out with a HAAS brand TM1 type CNC machine. CNC machine has 5.6 kW of power and a spindle speed of 4000 rpm. The experimental setup used in this study is illustrated in Fig. 2. Specifically, Fig. 2a presents a schematic picture of the experimental setup, while Fig. 2b shows the drill bits employed during the drilling process. Cutting fluid was used in the experiments. In the experiments, HSS and HSS+TiN coated drill bits were used. Three different feed rates (0.05, 0.10, and 0.15 mm/rev) and cutting velocities (15, 20, and 25 m/min) were tested to evaluate their performance under varying conditions. In this study, two different drill bits with a helix angle of 30° and a point angle of 118°, which are the most commonly used in the industry in terms of processing cost, were preferred. As a result of the literature review, 10 mm drill bit diameter was preferred as it is one of the preferred drill bit diameters in the experiments and shows more resistance to hard and abrasive SiC particles.

Table 1 — Chemical composition & Mechanical properties of Al-2024-T6 alloy

	Constituent	Content (%)
Chemical composition	Ti	0.049
	Zn	0.001
	Cr	0.018
	Fe	0.221
	Mn	0.689
	Si	0.077
	Mg	1.527
	Cu	4.581
	Al	Balance
	Mechanical properties	UTS (MPa)
Yield Strength (MPa)		324
Fracture Toughness, $K_{IC}$ (MPa-m <sup>1/2</sup> )		37
Elongation		21

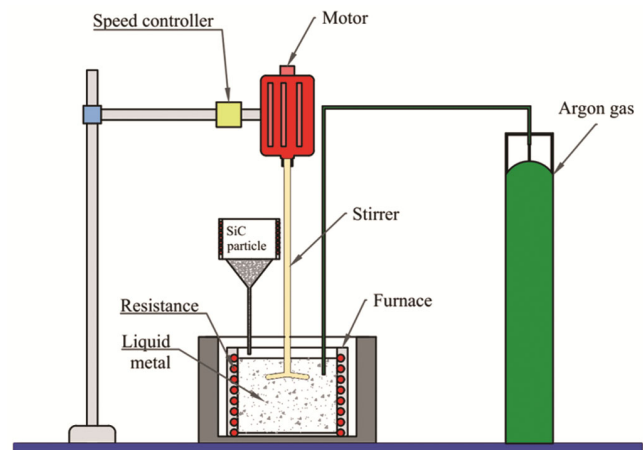


Fig. 1 — Stir casting procedure

**Experimental Design**

Taguchi Design is a design and optimisation methodology that focuses on optimising the durability and performance of developed products or processes. This method is often used in industrial production and engineering. This methodology enables the systematic testing of design factors and factor levels within a design of experiments. It is an experimental design in which many factors are evaluated simultaneously. These factors represent various parameters that affect product or process performance. The aim of Taguchi Design is to obtain a system that is more resistant to external factors that adversely affect system performance.

Therefore, the focus is usually on optimising the average effect and Signal-to-Noise Ratio (SNR). SNR is used as a metric to measure system performance. It is a measurement that expresses the ratio of the amount of information represented by a signal (S) to

the amount of noise (N) that distorts that signal. SNR is used to evaluate the quality of a signal and to indicate the level of unwanted noise in the signal. Another important use of SNR is in performance evaluation in experimental design and optimisation processes. For example, SNR used in Taguchi Design focuses on optimising factor levels to make the system more robust to external factors. In this case, SNR makes a measurement by combining the mean and variance of system performance and helps to determine optimal parameter settings. This use uses SNR to assess how close the system performance is to a desired aim.

The  $L_{18}$  orthogonal array, an example of Taguchi Design, is a design of experiments that allows factors and factor levels to be tested in a systematic way. This array represents a matrix containing 18 different combinations and each combination contains certain levels of factors. It also has only one interaction.  $L_{18}$  is often used in industrial experiments and product/process design optimisation. In this study, Minitab 21 package programme was used for Taguchi and ANOVA analysis. The  $L_{18}$  orthogonal array used for this study is given in Table 2.

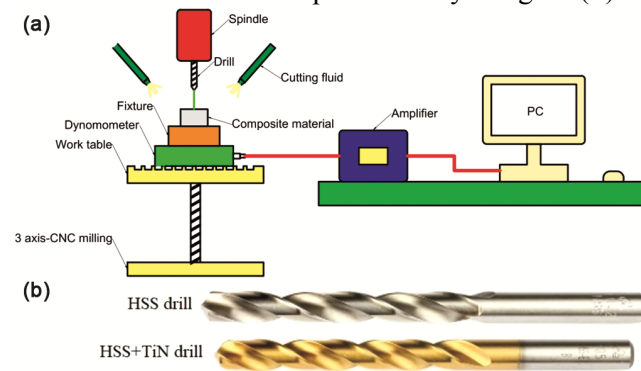


Fig. 2 — (a) Drilling set-up, (b) drill bits used

**Results and Discussion**

**Composite Production results**

After the composite production process, the test samples were subjected to metallographic sanding and polishing for microstructure examinations. Nikon Eclipse L150 A model optical microscope was used

Table 2 —  $L_{18}$  orthogonal array

Levels				Thrust force (N)	Torque (N.m)	SNR <sub>Thrust Force</sub>	SNR <sub>Torque</sub>
A	B	C	D				
1	1	1	1	7.06	0.78	-6.98	2.16
1	1	2	2	14.61	1.71	-23.29	-4.66
1	1	3	3	26.35	4.33	-28.42	-12.73
1	2	1	1	7.60	0.79	-17.62	2.05
1	2	2	2	16.12	1.98	-24.15	-5.93
1	2	3	3	28.15	4.42	-28.99	-12.91
1	3	1	2	13.97	1.65	-22.90	-4.35
1	3	2	3	24.32	4.32	-27.72	-12.71
1	3	3	1	12.05	1.50	-21.62	-3.52
2	1	1	3	7.13	1.34	-17.06	-2.54
2	1	2	1	4.03	0.72	-12.11	2.85
2	1	3	2	6.63	1.20	-16.43	-1.58
2	2	1	2	5.75	1.05	-15.19	-0.42
2	2	2	3	8.60	1.53	-18.69	-3.69
2	2	3	1	5.43	0.93	-14.70	0.63
2	3	1	3	7.57	1.47	-17.58	-3.35
2	3	2	1	5.40	0.87	-14.65	1.21
2	3	3	2	7.06	1.26	-16.98	-2.01

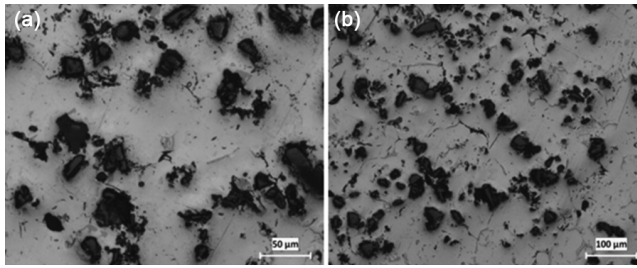


Fig. 3 — SiC particle structure distribution images in Al-2024 alloy: (a) 200X, (b) 100X magnification optical microscope images

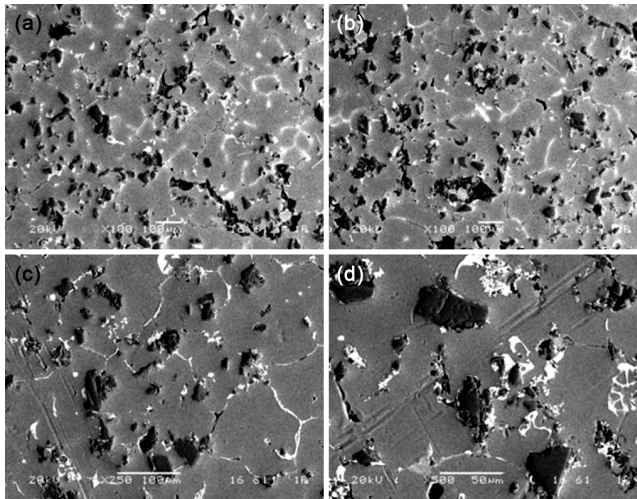


Fig. 4 — SEM images of 10% SiC reinforced Al-2024 alloy

for microstructure examinations of the prepared samples. The microstructure obtained from the optical microscope is shown in Fig. 3 where SiC reinforcement phases with hard and sharp corners are seen in black. When the SEM image of the 10% SiC particle reinforced Al2024 composite in Fig. 4 is utilised, superficial cracks are observed. In addition, it has been generally determined that it forms a smooth interface between the SiC particle and the Al-2024 matrix alloy. In addition, small gaps were observed. Finally, it is assumed that the SiC particles may have been broken during mixing with a mechanical mixer. T6 heat treatment was applied to the test samples produced by the Stir casting production method.

The hardness measurement results obtained at the end of the heat treatment process are given in Table 3. According to Table 3, the minimum hardness value was obtained in the Al-2024 matrix alloy and the maximum hardness value was obtained in the composite sample with a 15% SiC reinforcement phase. In addition, it was observed that the SiC reinforcement phases added to the Al-2024 matrix

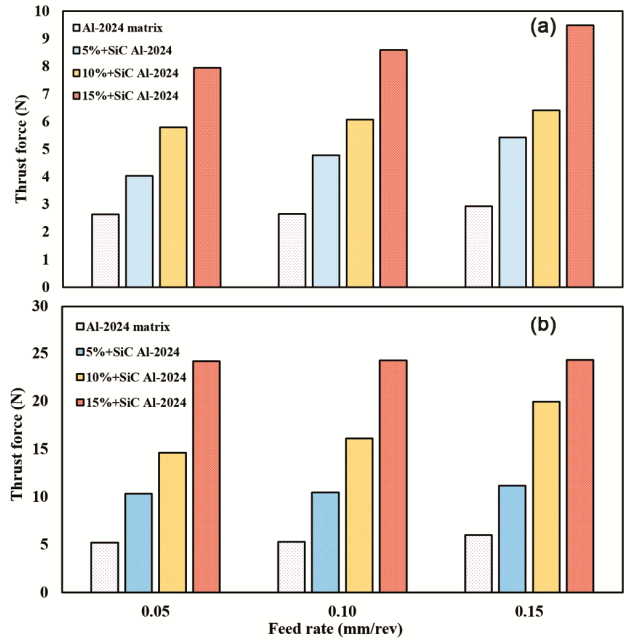


Fig. 5 — Variation of thrust force with feed rate at 20 m/min cutting velocity using: (a) HSS+TiN, (b) HSS drills

Table 3 — Hardness values of test materials

Material Type	Reinforcement Ratios (by volume)	Average Brinell Hardness (HB)
Al-2024 – T6	—	63
Al-2024 – T6	% 5 SiC	82
Al-2024 – T6	% 10 SiC	89
Al-2024 – T6	% 15 SiC	95

alloy had a positive effect on the hardness value of the composite material. This result was similar to the results in the literature.<sup>22-24</sup>

**Machinability Results**

Thrust force and torque results that occur during the drilling process are examined in terms of feed rate, cutting velocity, drill type, and material type. The thrust force variation with the feed rate at a cutting velocity of 20 m/min is depicted in Fig. 5. An examination of Fig. 5 reveals that thrust force increases as the feed rate rises for both types of drill bits. The lowest thrust force was observed at 0.05 mm/rev and the highest thrust force at 0.15 mm/rev. This can be explained in several ways. Firstly, the amount of material removed per revolution by the cutting tool and the effect of the reinforcement phase increase the thrust force with an increase in feed rate. Secondly, the increased feed rate increases the friction between the drill bit and the composite material. This causes an increase in the

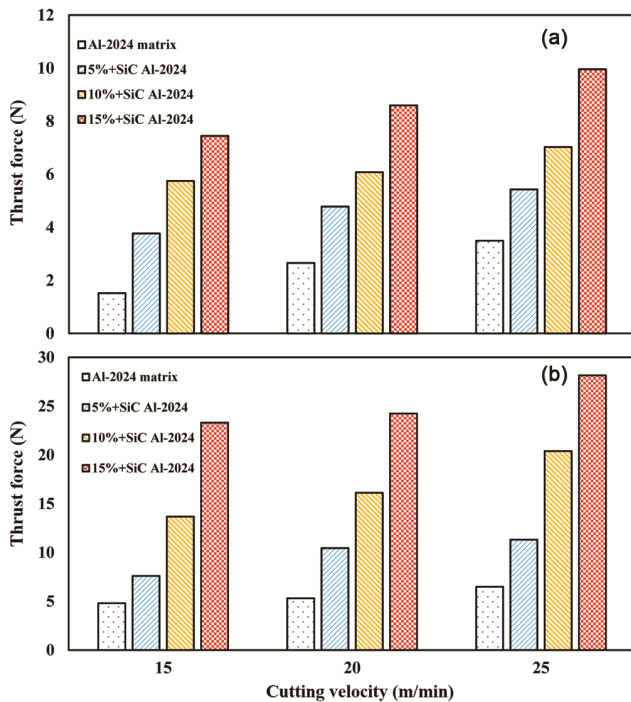


Fig. 6 — Variation of thrust force with cutting velocity at 0.10 mm/rev feed rate using: (a) HSS+TiN (b) HSS drills

Volume of Material Removed (MRR) and an excessive increase generates thrust force.<sup>25</sup>

The change in thrust force with increasing cutting velocity at 0.10 mm/rev is shown in Fig. 6. It is clear from this figure that the thrust force increased with increasing cutting velocity for both drill bits. During the drilling process, friction occurs between the drill bit and the composite workpiece. As the cutting speed increases, the heat of friction causes an increase in temperature at the interface. This temperature increase harms the drill bit. This negative effect can increase the deformation and/or wear of the drill bit. In this case, an increase in cutting forces can be seen. In addition, drilling length affects drill bit wear and can cause increased cutting forces. This phenomenon is similar to Lin and Chen's work.<sup>26</sup>

In addition, high cutting speeds can increase the temperature of the composite material during the drilling process. This can lead to a change in the coefficient of thermal expansion of the composite. In particular, SiC has a different coefficient of thermal expansion than aluminum. This thermal mismatch can affect the cutting forces. In this case, it can lead to the formation of voids in the composite material due to the displacement of the SiC particle or the formation of cracks in the matrix material. This can increase the cutting forces and lead to the formation of holes.

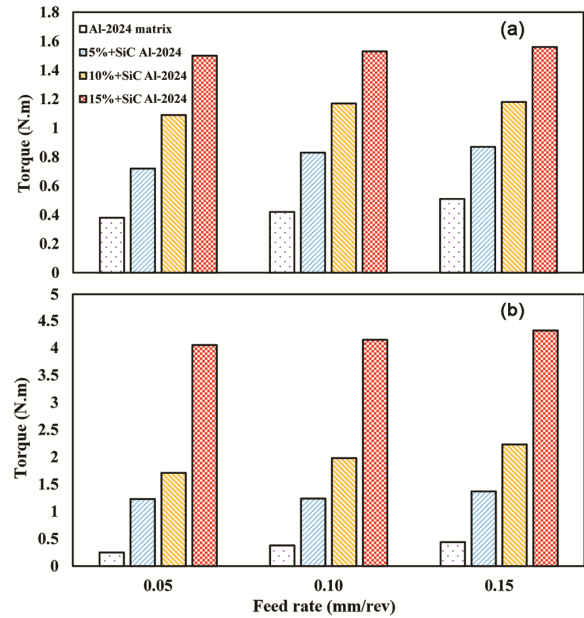


Fig. 7 — Variation of torque with feed rate at 20 m/min cutting velocity using: (a) HSS+TiN, (b) HSS drills

Finally, high cutting speeds can also affect surface quality. The chips generated during drilling can become difficult to manage and it is also possible that the chips can damage the material surface.<sup>27</sup>

The change in torque with the increase of the feed rate at 20 m/min cutting velocity is shown in Fig. 7. According to Fig. 7, it was observed that thrust force increased with the increase in the feed rate for both HSS + TiN and HSS drill bits. At the drilling condition of 0.10 mm/rev, approximately 1.6 N torque was obtained in the HSS + TiN drill bit, while approximately 4 N was obtained in the HSS drill bit. The HSS + TiN drill bit has 150% less torque than the HSS drill bit.

When the force graphs of the drill bits used in this study were analysed in terms of material, it was observed that TiN coated HSS drill bits performed better than uncoated HSS drill bits. This is due to the fact that TiN coating provides high hardness and wear resistance on the cutting tool. Due to the heat generated between the drill bit and the composite material during the drilling process, TiN coated HSS drill bits are thought to provide longer life and less wear of the cutting tool compared to HSS due to these properties. As a result, less torque is required when drilling SiC particle reinforced Al+2024 composite material.<sup>28</sup>

The change in torque value for both drill bits with an increase in cutting velocity at a feed rate of 0.10 mm/rev is shown in Fig. 8. From this figure it is

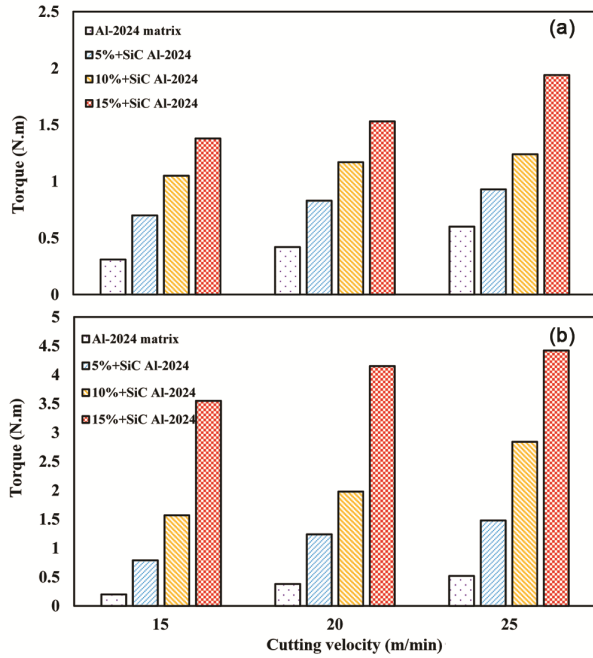


Fig. 8 — Variation of torque with cutting velocity at 0.10 mm/rev feed rate using: (a) HSS+TiN, (b) HSS drills

observed that torque value increases with the increase of cutting velocity in both drill bits. This situation was similar to other studies in the literature.<sup>29–31</sup>

Analysis of Figs. 5–8 reveals that an increase in SiC particles leads to a rise in both thrust force and torque. This situation can be explained in many ways. SiC particles provide high hardness and wear resistance in the metal matrix. However, this hardness causes a higher load on the tool during the drilling process. High torque is required to overcome these high loads. Secondly, chip formation and cutting forces play an important role during drilling of MMC materials. Abrasive and hard SiC particles can make chip formation difficult and increase cutting forces. Lastly, in materials with higher SiC percentage, it may be necessary to use more durable and sharp tools. Therefore, these tools must have the appropriate cutting-edge geometry to operate with higher torque.<sup>32</sup> Liu *et al.* determined that in the dry drilling of SiCp/Al composites, the particle volume fraction (Pvf) significantly affects the cutting force, burr height, and surface roughness, and that the chip and burr structure at the hole exit changes as Pvf increases.<sup>33</sup>

**Statistical Analysis Results**

In Taguchi Design, the quality characteristic "Smaller is Better" usually refers to situations where the minimum value represents the desired state. In this

case, the goal of quality improvement is to keep the value as low as possible. A typical performance measurement formula for the "Smaller is Better" quality characteristic is as follows:

$$\frac{S}{N} = -10 \log \frac{1}{n} (\sum y^2) \quad \dots (1)$$

where, n indicates the number of experiments and yi indicates the experimental data. The results in Table 2 can be used to calculate the mean SNR for each of the levels in each variable. The average SNR plots corresponding to various values of variables A, B, C, and D for both thrust and torque are presented in Fig. 9. The order of the selected variables' efficiency can be determined from the value changes shown in this figure. This indicates that variable A (the drill), will have the most impact on the thrust force out of the four variables examined in this study. The analysis of Fig. 9a identifies A<sub>2</sub>B<sub>1</sub>C<sub>1</sub>D<sub>1</sub> as the optimal test parameter for minimizing thrust force, an observation further supported by the surface map in Fig. 10a. Similarly, Fig. 9b illustrates the average SNR plot for torque across various values of variables A, B, C, and D, confirming that A<sub>2</sub>B<sub>1</sub>C<sub>1</sub>D<sub>1</sub> is also the ideal parameter for achieving the lowest torque value. This conclusion is further validated by the torque surface map presented in Fig. 10b. The A × B interaction plot for both thrust and torque is shown in Fig. 11a and b.

The ANOVA (Analysis of Variance) table is a table that summarizes the results of an ANOVA analysis. This table is used to evaluate differences between groups and determine whether they are statistically significant. F<sub>value</sub> must be greater than 4 for the variance to have a significant effect on the result.<sup>34</sup> The ANOVA table for thrust and torque analyses is presented in Table 4. Accordingly, A, C, and D are variables that significantly affect both the thrust force and the torque. According to the ANOVA table obtained in Table 4 for thrust force, the most effective variable was variable A (Drill) with 58.36%, followed by variable D (Composite) with 31.25% and variable C (cutting velocity) with 7.64%. Similarly, it is observed from the ANOVA Table obtained for torque that the most effective variable is variable D (Composite) with 55.84%, followed by variable A (Drill) with 24.96% and variable C (cutting velocity) with 13.26%, respectively. It was also observed that the A×B interactions for both thrust and torque are very small and can be ignored. The ANOVA results were consistent with those obtained with the Taguchi L18 array based on the signal-to-noise ratio (Table 5).

Regression analysis is a statistical analysis method used to understand the relationship between two or more variables and to evaluate how one variable affects the other. Basically, it tries to model the relationship between the dependent variable and one or more independent variables. Regression analysis is often used to predict the dependent variable or to

understand the effects of controlling independent variables. The  $R^2$  coefficient for multiple linear regression is 0.8 to 1.<sup>(35)</sup> The mathematical equations obtained by regression analysis for thrust force and torque are given in Table 6. The mathematical equations allow you to calculate predicted thrust force and torque values for each test.

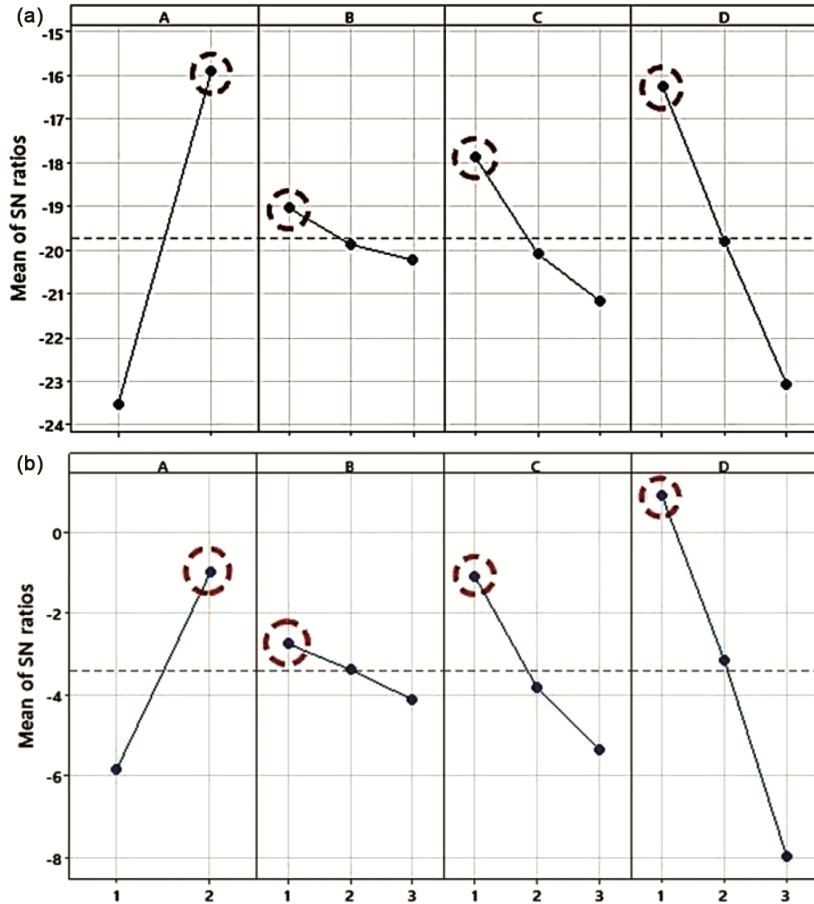


Fig. 9 — Main effect plot of SN ratio data means on: (a) the thrust force, (b) the torque

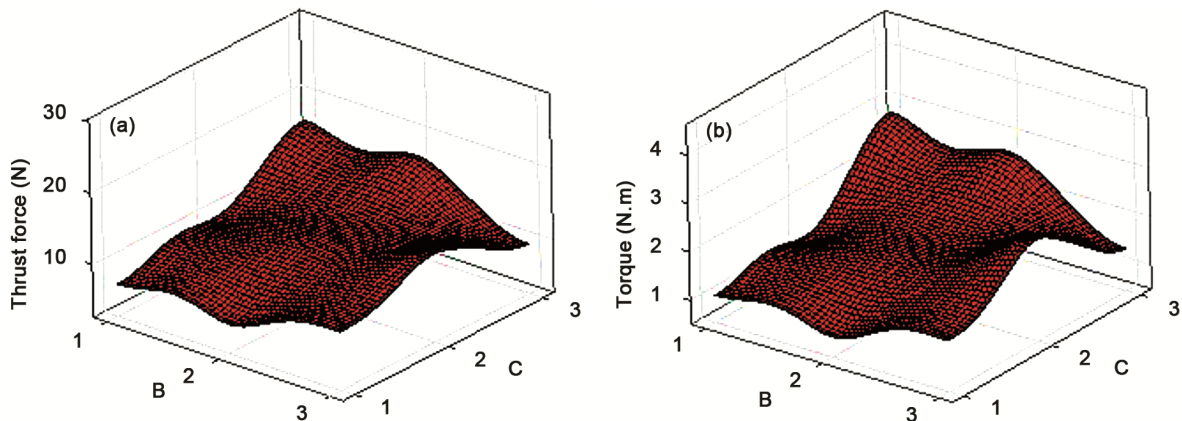


Fig. 10 — Surface map of: (a) the thrust force, (b) the torque

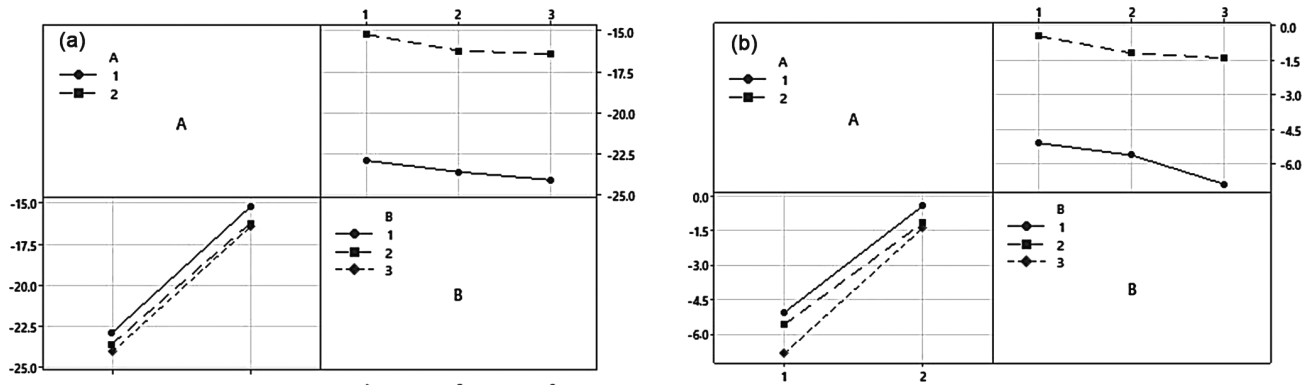


Fig. 11 — Interaction plot for SN ratio of A×B data means of: (a) the thrust force, (b) the torque

Table 4 — ANOVA for different parameters

Source	DF	Adj SS	Adj MS	F-Value	F-Table	P(%)
Thrust force						
A	1	259.141	259.141	271.62	11.26 <sup>a</sup>	58.36
B	2	4.518	2.259	2.37		1.02
C	2	33.914	16.957	17.77	8.65 <sup>a</sup>	7.64
D	2	138.780	69.390	72.73	8.65 <sup>a</sup>	31.25
A*B	2	0.088	0.044	0.05		0.02
Error	8	7.632	0.954			
Total	17	444.074				
Torque						
A	1	106.110	106.110	45.40	11.26 <sup>a</sup>	24.96
B	2	5.645	2.822	1.21		1.33
C	2	56.365	28.182	12.06	8.65 <sup>a</sup>	13.26
D	2	237.402	118.701	50.79	8.65 <sup>a</sup>	55.84
A*B	2	0.909	0.455	0.19		0.21
Error	8	18.696	2.337			
Total	17	425.127				

<sup>a</sup>Confidence level is 99%

Table 5 — Response tables for thrust force and torque

Level	Thrust force				Level	Torque			
	A	B	C	D		A	B	C	D
1	-3.52	-19.05	-17.89	-16.28	1	-58.45	-27.51	-10.76	0.90
2	-15.93	-19.89	-20.10	-19.82	2	-0.99	-33.80	-38.22	-31.60
3		-20.24	-21.19	-23.08	3		-41.21	-53.54	-79.88
Delta	7.59	1.19	3.30	6.80	Delta	48.56	13.70	42.77	88.85
Rank	1	4	3	2	Rank	2	4	3	1

Table 6 — The mathematical equations for the thrust force and torque

Thrust Force (N) =  $-19.726 - 3.794*A_1 + 3.794*A_2 + 0.679*B_1 - 0.163*B_2 - 0.516*B_3 + 1.837*C_1 - 0.375*C_2 - 1.462*C_3 + 3.449*D_1 - 0.098*D_2 - 3.351*D_3 - 0.053*A*B_{11} + 0.099*A*B_{12} - 0.045*A*B_{13} + 0.053*A*B_{21} - 0.099*A*B_{22} + 0.045*A*B_{23}$   
 $R^2 = 98.28\%$

Torque (N.m) =  $-3.417 - 2.428*A_1 + 2.428*A_2 + 0.667*B_1 + 0.037*B_2 - 0.704*B_3 + 2.341*C_1 - 0.405*C_2 - 1.936*C_3 + 4.313*D_1 + 0.258*D_2 - 4.571*D_3 + 0.101*A*B_{11} + 0.210*A*B_{12} - 0.312*A*B_{13} - 0.101*A*B_{21} - 0.210*A*B_{22} + 0.312*A*B_{23}$   
 $R^2 = 95.60\%$

**Conclusions**

This study successfully developed Al2024 composites using the stir casting process, highlighting their potential in the aviation sector. The addition of

SiC particles increased the material's hardness, while HSS+TiN-coated drill bits outperformed HSS bits in all performance tests. Higher cutting speeds and feed rates led to increased torque and thrust force. The

Taguchi method effectively optimized drilling parameters, with  $A_2B_1C_1D_1$  identified as the best combination for minimizing cutting forces. ANOVA revealed that drill type had the most significant impact on thrust force (58.36%), followed by composite type (31.25%) and cutting speed (7.64%). For torque, composite type influenced 55.94%, drill type 24.96%, and cutting speed 13.26%. The study's limitations include its specific material focus and controlled experimental settings. Future research could explore alternative reinforcements, advanced surface treatments, and extended parameter ranges to further enhance machinability and broaden application potential.

## References

- Erdemir F, Canakci A & Varol T, Microstructural characterization and mechanical properties of functionally graded Al2024/SiC composites prepared by powder metallurgy techniques, *Trans Nonferrous Met Soc China* (English Ed), **25** (2015) 3569–3577, [https://doi.org/10.1016/S1003-6326\(15\)63996-6](https://doi.org/10.1016/S1003-6326(15)63996-6).
- Li Z, Zhang Y, Xiong H, Kong C & Yu H, Fabrication of particle-reinforced aluminum alloy composite: role of casting and rolling, *Mater Manuf Process*, **37(1)** (2021) 90–98, <https://doi.org/10.1080/10426914.2021.194419>.
- Singh J & Chauhan A, Fabrication characteristics and tensile strength of novel Al2024/SiC/red mud composites processed via stir casting route, *Trans Nonferrous Met Soc China* (English Ed), **27** (2017) 2573–2586, [https://doi.org/10.1016/S1003-6326\(17\)60285-1](https://doi.org/10.1016/S1003-6326(17)60285-1).
- Choudhary R, Kumar A, Raj H, Kumar S, Tiwari S, Khan S & Sharma V, Fabrication and characterization of stir cast Al2024/SiCp metal matrix composite, *Mater Today Proc*, **26** (2019) 3316–3320, <https://doi.org/10.1016/j.matpr.2020.02.471>.
- Parikh V K, Badheka V J, Badgujar A D & Ghetiya N D, Fabrication and processing of aluminum alloy metal matrix composites, *Mater Manuf Process*, **36(14)** (2021) 1604–1617, <https://doi.org/10.1080/10426914.2021.1914848>.
- Parikh V K, Badgujar A D & Ghetiya N D, Investigation of microstructural and wear properties of stir cast and friction stir processed AA 2014-based metal matrix composites, *Adv Mater Process Technol*, **9(4)** (2022) 1920–1940, <https://doi.org/10.1080/2374068X.2022.2136688>.
- Jawalkar C S & Kant S, A review on use of aluminium alloys in aircraft components. i-manager's, *J Mater Sci*, **3** (2015) 33–38, <https://doi.org/10.26634/jms.3.3.3673>.
- Dey D & Biswas A, Comparative study of physical, mechanical and tribological properties of Al2024 Alloy and SiC-TiB2 Composites, *Silicon*, **13** (2021) 1895–1906, <https://doi.org/10.1007/s12633-020-00560-9>.
- Verma B B, Atkinson J D & Kumar M, Study of fatigue behaviour of 7475 aluminium alloy, *Bull Mater Sci*, **24** (2001) 231–236, <https://doi.org/10.1007/BF02710107>.
- Dursun T & Soutis C, Recent developments in advanced aircraft aluminium alloys, *Mater Des*, **56** (2014) 862–871, <https://doi.org/10.1016/j.matdes.2013.12.002>.
- Chang L, Weiwei X, Yan Xiaogeng J & Tao Y, Mechanistic force modeling in drilling of SiCp/Al matrix composites considering a comprehensive abrasive particle model, *Int J Adv Manuf Technol*, **109** (2020) 421–442.
- Zhu C, Wu Y Gu P, Tao Z & Yu Y, Prediction of drilling force for high volume fraction SiCp/Al composite based on neural network, *Procedia, CIRP* **99** (2021) 414–419.
- Abbas C A, Chuanzhen H, Hafeez H, Binghao L & Hanlian L, Influence of cryogenic treatment duration of drills on drilling performance and hole quality of metal matrix composite materials, *J Mech Sci Technol*, **37** (2023) 5081–5091. <https://doi.org/10.1007/s12206-023-0913-8>.
- Ghalme S G & Karolczak P, Optimization of drilling parameters for aluminum metal matrix composite using entropy-weighted TOPSIS under MQL conditions, *Eng Transac*, **71(4)** (2023) 595–616 <https://doi.org/10.24423/EngTrans.3110.20231121>.
- Sharath B N, Karthik S, Pradeep D G, Madhu K S & Venkatesh C V, Machinability studies on boron carbide and graphite reinforced Al7029-Based hybrid composites, in *Materials, Design and Manufacturing for Sustainable Environment-Lect Notes Mech Eng*, edited by E Natarajan, S Vinodh, V Rajkumar (Springer, Singapore) 2023, [https://doi.org/10.1007/978-981-19-3053-9\\_38](https://doi.org/10.1007/978-981-19-3053-9_38).
- Umer U, Mohammed M K, Abidi M H, Alkhalefah H & Kishawy H A, Machinability analysis and multi-response optimization using NGS-II algorithm for particle reinforced aluminum based metal matrix composites, *Adv Prod Eng Manag*, **17** (2022) 205–218.
- Yildiz T & Sur G, Investigation of drilling properties of AA7075/Al2O3 functionally graded materials using gray relational analysis, *Proc Inst Mech Eng Part B*, **235(9)** (2021) 1384–1398, doi: 10.1177/0954405421995657.
- Selvamani M, Balu G, Ellapan B & Raja D, Processing of powder metallurgy metal matrix composite and performance analysis during machining, *AIP Conf Proc* **7**, **2766(1)** (2023) 020011, <https://doi.org/10.1063/5.0139439>.
- Xiang J, Pang S, Xie L, Gao F, Hu X, Yi J & Hu F, Mechanism-Based FE simulation of tool wear in diamond drilling of SiCp/Al composites, *Mater*, **11(2)** (2018) 252, <https://doi.org/10.3390/ma11020252>.
- Dewei L, Changhe L, Peiming X, Wei W, Yanbin Z, Min Y, Xin C, Benkai L, Mingzheng L, Teng G, Yusuf Suleiman D & Aiguo Qin, SiCp/Al composites from conventional to empowered machining: Mechanisms and processability, *Compos Struct*, **346** (2024) 118433, <https://doi.org/10.1016/j.compstruct.2024.118433>.
- Ficici F, Evaluation of surface roughness in drilling particle-reinforced composites, *Adv Compos Lett*, **29** (2020) 2633366X2093771, <https://doi.org/10.1177/2633366X20937711>.
- Ye T, Xu Y & Ren J, Effects of SiC particle size on mechanical properties of SiC particle reinforced aluminum metal matrix composite, *Mater Sci Eng A*, **753** (2019) 146–155.
- Liu P, Wang A, Xie J & Hao S, Effect of heat treatment on microstructure and mechanical properties of SiCp/2024 aluminum matrix composite, *J Wuhan Univ Technol Sci Ed*, **30(6)** (2015) 1229–1233.
- Arvind M S, Kaushik M P, Mayur A M, Khaled G, Danil Y P, Wojciechowski S & Khanna N, Effect of mixing method and

- particle size on hardness and compressive strength of aluminium based metal matrix composite prepared through powder metallurgy route, *J Mater Res Technol*, **18** (2022) 282–292, <https://doi.org/10.1016/j.jmrt.2022.02.094>.
- 25 Karnam M, Shivaramakrishna A, Joshi R, Manjunatha T H, Veerabhadrapa K, Study of Mechanical Properties and Drilling Behavior of Al7075 Reinforced with B<sub>4</sub>C, *Mater Today Proc*, **5** (2018) 25102–25111, <https://doi.org/10.1016/j.matpr.2018.10.311>.
- 26 Lin S C & Chen I K, Drilling carbon fiber-reinforced composite material at high speed, *Wear*, **194** (1996) 156–162, [https://doi.org/10.1016/0043-1648\(95\)06831-7](https://doi.org/10.1016/0043-1648(95)06831-7).
- 27 Bhardwaj A R, Vaidya A M & Shekhawat S P, Machining of aluminium metal matrix composite: a review, *Mater Today Proc*, **21** (2020) 1396–402, <https://doi.org/10.1016/j.matpr.2020.01.179>.
- 28 Ghinatti E, Bertolini R, Sorgato M, Ghiotti A & Bruschi S, Tool wear and surface finish analysis after drilling Al-SiC metal matrix composite with DLC-coated tools at varying feed, *Procedia CIRP*, **123** (2024) 53–58, <https://doi.org/10.1016/j.procir.2024.05.012>.
- 29 Giasin K, Hodzic A, Phadnis V & Ayvar-Soberanis S, Assessment of cutting forces and hole quality in drilling Al2024 aluminium alloy: experimental and finite element study, *Int J Adv Manuf Technol*, **87** (2016) 2041–2061, <https://doi.org/10.1007/s00170-016-8563-y>.
- 30 Xavier L F & Suresh P, Drilling studies on the prepared aluminum metal matrix composite from wet grinder stone dust particles, *IEEE J Sel Top Quantum Electron*, **25** (2018) 473–487, <https://doi.org/10.1515/secm-2016-0040>.
- 31 Taşkesen A & Kütükde K, Experimental investigation and multi-objective analysis on drilling of boron carbide reinforced metal matrix composites using grey relational analysis, *Meas J Int Meas Confed*, **47** (2014) 321–330, <https://doi.org/10.1016/j.measurement.2013.08.040>.
- 32 Abbas C A, Huang C, Binghao L & Hanlian L, Research on cryogenic high-speed drilling performance of metal matrix composite materials (Al/SiC) using cryogenically treated drills, *J Braz Soc Mech Sci Eng*, **46** (2024) 448, <https://doi.org/10.1007/s40430-024-05007-5>.
- 33 Liu C, Li C, Xu W & Gao L, Variation characteristics of machinability in drilling of SiC particle reinforced aluminum matrix (SiCp/Al) composite with a wide range of particle volume fractions, *Int J Adv Manuf Technol*, **121** (2022) 6285–6302, <https://doi.org/10.1007/s00170-022-09731-x>.
- 34 Fıccı F, Investigation of wear mechanism in the drilling of PPA composites for the automotive industry, *J Eng Res*, **11**(2023) 100034, <https://doi.org/10.1016/j.jer.2023.100034>.
- 35 Fıccı F, Investigation of thrust force in drilling polyphthalamide (PPA) composites, *Meas J Int Meas Confed*, **182** (2021) 109505, <https://doi.org/10.1016/j.measurement.2021.109505>.